ARTICLE

OBC
www.rsc.org/obc

Barriers to internal rotation around the C–N bond in 3-(*o*-aryl)-5-methyl-rhodanines using NMR spectroscopy and computational studies. Electron density topological analysis of the transition states

Yeliz Aydeniz,[a] Funda Oğuz,[a] Arzu Yaman,[a] Aylin Sungur Konuklar,[a] Ilknur Doğan,[a] Viktorya Aviyente*[a] and Roger A. Klein[b]

[a] *Department of Chemistry, Boğazici University, Bebek, Istanbul, Turkey. E-mail: aviye@boun.edu.tr*

[b] *Institute for Physiological Chemistry, University of Bonn, Germany. E-mail: klein@institut.physiochem.uni-bonn.de*

Received 4th May 2004, Accepted 2nd July 2004
First published as an Advance Article on the web 4th August 2004

We have investigated the pairs of rotational isomers for six 3-(*o*-aryl)-5-methyl-rhodanines (Z = H, F, Cl, Br, OH, and CH_3) using NMR spectroscopy and density functional theory (DFT) calculations. Electron density topological and NBO analysis has demonstrated the importance of non-covalent interactions, characterised by (3, −1) bond critical points (BCPs), between the oxygen and sulfur atoms on the thiazolidine ring with the aryl substitutents in stabilizing the transition states. The energetic activation barriers to rotation have also been determined using computational results; rotational barriers for 3-(*o*-chlorophenyl)-5-methyl-rhodanine (**3S**) and 3-(*o*-tolyl)-5-methyl-rhodanine (**6S**) were determined experimentally based on NMR separation of the diastereoisomeric pairs, and the first-order rate constants used to derive the value of the rotational barrier from the Eyring equation.

Introduction

Thiazolidinediones and rhodanines are known to possess pharmacological activity[1] and to be very effective in improving glycaemic control in diabetic patients, potentiating the action of insulin and thus lowering blood glucose levels. Rhodanines have both antiviral and antibacterial activity.[2] The 3-(*o*-aryl)-5-methyl-rhodanines that we have analysed consist of a five-membered ring bonded to a phenyl ring, *i.e.* a 5/6 ring skeleton (Fig. 1).

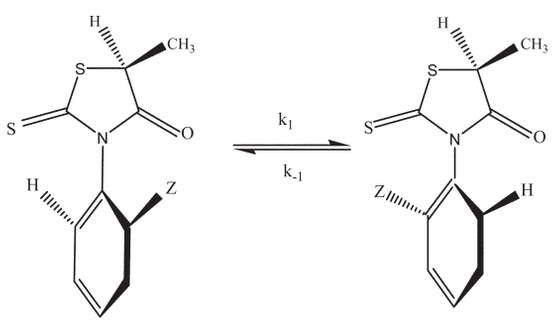

Fig. 1 Hindered internal rotation around the C_{aryl}–N_{sp^2} bond in *ortho*-aryl-substituted rhodanines.

The existence of hindered rotation around C–C single bonds has drawn attention to the potential energy surfaces of these compounds. Although in the late 1910s it was thought that free rotation could occur around any carbon–carbon single bonds, as time passed evidence was obtained that free rotation was hindered in many compounds and that these molecules existed as equilibrium mixtures of a number of preferred rotational isomers.[3] The hindered rotation around the C–N bond of the 3-(*o*-aryl)-rhodanines can be thought of as representing a model for the rotational equilibrium around the C–N bond in 5/6 ring skeletons (Fig. 1).

The compounds studied are shown in Fig. 2. The Z group represents the substituents, *i.e.* H, F, Cl, Br, OH, or CH_3. It is known that rotation about the *N*-(phenyl) bond is restricted both by the size of the *ortho*-substituent and the presence of an exocyclic S and O, causing a rotational barrier between the stereoisomers **S**–**P**/**S**–**M** and **R**–**M**/**R**–**P** (Fig. 1). The most obvious way of explaining the appearance of a potential barrier resulting in hindered rotation is to carry out an *ab initio* quantum-mechanical calculation of the total energy of the molecule as a function of the dihedral angle, at a sufficiently high level of theory. The difference between neighbouring maxima and minima is the energy barrier during hindered rotation. In the ground state the two ring systems are orthogonal to one another, or very nearly so. There are two transition states with geometries corresponding to the Z group on the same side or opposite side to the carbonyl or thiocarbonyl group with the two ring systems nearly coplanar, such that rotation is sterically hindered. These compounds possess both a chiral centre and a chiral axis; the chiral centre is the methyl-substituted carbon atom C5 and the C–N bond forms the chiral axis. Thus, four stereoisomers, **S**–**P**, **S**–**M**, **R**–**M** and **R**–**P**[4] coexist as shown in Fig. 1. **S**–**P**/**R**–**M** and **S**–**M**/**R**–**P** are enantiomeric pairs, whereas **S**–**P**/**S**–**M** and **R**–**M**/**R**–**P** are diastereomers interconvertible through 180° rotation around the C–N bond. In this study, sulfur-containing compounds (rhodanine derivatives) with **S**–**P** and **S**–**M** configurations have been modelled computationally.

The *N*-aryl-2-thioxo-4-oxazolidinones, as well as *N*-(*o*-aryl)-rhodanines with CH_3 and Cl substituents, have been synthesized and the barriers to rotation by thermal racemization determined by Dogan *et al*.[5] A study by Colebrook[6] investigated conformational isomerism in 1-aryl, 3-aryl and 3-aryl-2-thio-hydantoins with H, F, Cl, Br, CH_3 substituents. They found stationary points at 50° and 120° with a small barrier at 90°. The transition states observed at 0° and 180° are higher in energy compared to the transition state at 90°. The influence of F, Cl, Br, NH_2, and OCH_3 substituents on the rotational energy barrier for 2,2-disubstituted biphenyls has been studied by König *et al.* and dynamic gas chromatography has been used to determine the energy barriers for atropisomeric biphenyls.[7,8] In 1997, Cui *et al.*[9] reported studies on aromatic polyimides with 6/6 and 5/6 ring systems. They found the minimum energy conformers for these two adjoining ring systems at 90° and 46° using MP2 (Møller-Plesset-2) and HF (Hartee–Fock) methods, respectively. In 1998, Rang *et al.*[10] described studies of the stereochemistry and conformational analysis of 3-(alkyl)- or 3-(aralkyl)-5-(methyl/phenyl)-rhodanines using X-ray crystallography, UV spectroscopy and molecular mechanics.

DOI: 10.1039/b406556e

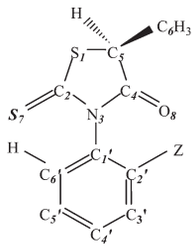

Compound	Name	Z
1S	3-(phenyl)-5-methyl-rhodanine	H
2S	3-(*o*-fluorophenyl)-5-methyl-rhodanine	F
3S	3-(*o*-chlorophenyl) 5-methyl-rhodanine	Cl
4S	3-(*o*-bromophenyl)-5-methyl-rhodanine	Br
5S	3-(*o*-hydroxyphenyl)-5-methyl-rhodanine	OH
6S	3-(*o*-tolyl)-5-methyl-rhodanine	CH_3

Fig. 2 Atom numbering and the compound naming for 3-(*o*-aryl)-5-methyl-rhodanines.

In this paper, we focus on the conformational behaviour of the 3-(*o*-aryl)-5-methyl-rhodanines with H, F, Cl, Br, OH, CH_3 substituents. The CH_3 and Cl derivatives have been synthesized and the barriers to rotation have been determined experimentally. Rationalisation of the effect of substituents on the hindered rotation, together with DFT calculations followed by electron density topological analysis of the wavefunction, enables us to understand better the nature of the interactions present in each compound and their transition states. Comparison of the computational results with the experimental observations provides support for the conclusions drawn.

Methodology

Experimental

3-(*o*-Chlorophenyl)-5-methyl-rhodanine, 3S, was synthesized by reacting ammonium *o*-chlorophenyl dithiocarbamate, prepared from 0.3 mol of CS_2 and 0.2 mol *o*-chloroaniline in 25% ammonia solution, with the sodium salt of 2-chloropropionic acid (0.15 mol) in aqueous sodium hydroxide solution.[11] The product was purified by column chromatography over silica using 1 : 3 v/v $CHCl_3$/petroleum ether as the eluting solvent (1.25 g, 3%), mp 93 °C. (Found: C, 47.46; H, 3.28; N, 5.39%. Calc. for $C_{10}H_8NOS_2Cl$: C, 46.60; H, 3.11; N, 5.43%). δ_H (250 MHz; C_6D_6; Me_4Si) 3.40, 3.54 [H, quartet, J = 7.3, 7.3, C(5)H, one for each diastereomer], 1.07, 1.19 [3 H, doublet, J = 7.3, 7.3, C(5)Me, one for each diastereomer], 7.22–7.58 (4 H, multiplet, Ph); δ_C (62.5 MHz; C_6D_6; Me_4Si) 198.8 (thiocarbonyl carbon in heterocycle), 175.4 (carbonyl carbon in heterocycle) 46.0, 45.8 (methine carbon in heterocycle, one for each diastereomer), 18.5, 17.5 (methyl carbon attached to C-5 of the heterocycle, one for each diastereomer), 133.4, 132.8, 130.8, 130.2, 127.7 (aromatic carbons).

3-(*o*-Tolyl)-5-methyl-rhodanine, 6S, was synthesized by reacting racemic ethylthiolactate (0.02 mol) with *o*-tolylisothiocyanate (0.02 mol) in the presence of a catalytic amount of sodium metal in toluene.[11] At the end of 5 h of refluxing, toluene was removed by evaporation and the product purified by recrystallization from a petroleum ether–ethanol mixture (1.8 g, 33%), mp 81 °C. (Found: C, 55.98; H, 4.83; N, 5.76%. Calc. for $C_{11}H_{11}NOS_2$: C, 55.70; H, 4.64; N, 5.90%). δ_H (250 MHz; C_6D_6; Me_4Si) 3.36, 3.43 [1 H, quartet, J = 7.3, 7.3, C(5)H, one for each diastereomer], 1.08, 1.11 [3 H, doublet, J = 7.3, 7.3, C(5)Me, one for each diastereomer], 1.88, 1.94 (3 H, singlet, *o*-Me, one for each diastereomer), 6.79–7.00 (4 H, multiplet, Ph); δ_C (62.5 MHz; C_6D_6; Me_4Si) 176.2 (carbonyl carbon in heterocycle) 45.7 (methine carbon in heterocycle), 18.5, 17.3 (methyl carbon attached to C-5 of the heterocycle, one for each diastereomer), 18 (*o*-Me), 135.2, 136.5, 131.3, 129.9, 129.1, 127.3 (aromatic carbons).

^{1}H and ^{13}C NMR spectra were recorded on a Bruker AC-250 (250 MHz, 20 °C) spectrometer, 2D-NOESY spectra were taken on a Varian-Mercury (VX-400 MHz-BB, 30 °C) spectrometer. J values are given in Hz. Melting points were recorded using Fisher Johns melting point apparatus. Elemental analyses were performed on Carlo Erba 1100. Thermal interconversion studies have been done keeping the sample in the NMR cavity at a constant temperature (sensitivity is ±0.1) and recording the spectra over time.

Computational

The potential energy surface for free rotation around the C1′–N3 bond of the 3-(*o*-aryl)-5-methyl-rhodanines with H, F, Cl, Br, OH and CH_3 *ortho*-substituents on the aryl ring was sampled in each case with PM3 using the SPARTAN 5.1.1 package.[12] The local minima and the transition structures located with PM3 were then optimized at the B3LYP/6-31G* level using Gaussian-98.[13] Vibrational frequency analysis was carried out in order to confirm the nature of the stationary points. The vibrational frequencies have been utilized to calculate the zero-point energy (ZPE) and thermal energy corrections. Wavefunction files were generated in Cartesian coordinates using the Gaussian option 6D 10F; the use of the option scf = tight was important to prevent 'charge leakage' as described by Popelier.[14] Electron density topology was analysed using Biegler-König's AIM2000 and Popelier's MORPHY98 programs.[14,15] Natural bond orbital (NBO) theory was applied to selected compounds in order to understand their structural features.[16] For the compounds modelled, the stereocenter C5 had the **S**-configuration and structures are denoted as **S**–**M** with the C4–N3–C1′–C2′ dihedral angle positive, or as **S**–**P** with the C4–N3–C1′–C2′ dihedral angle negative. The acronyms **TS** and **TS′** refer to the transition structures where the substituent interacts with oxygen or sulfur respectively (Fig. 2).

Results and discussion

Experimental

Experimental determination of the rotational barriers was carried out for 3-(*o*-tolyl)-5-methyl-rhodanine (**6S**) and 3-(*o*-chlorophenyl)-5-methyl-rhodanine (**3S**). Synthesis yielded a mixture of the four stereoisomers, **S**–**M**, **S**–**P**, **R**–**M** and **R**–**P** (Fig. 1). The ^{1}H NMR spectrum consisted of superimposed spectra for two diastereomers, one for the **S**–**M**/**R**–**P** enantiomeric pair and one for the **S**–**P**/**R**–**M** pair. In the case of 3-(*o*-tolyl)-5-methyl-rhodanine, the ratio of the diastereomers was found to be 1 : 3.2, based on the signal intensities of the well resolved *ortho*-methyl signals (Fig. 3a). When this isomeric mixture was kept at constant temperature and the ^{1}H NMR spectrum recorded over time, the intensity of the lower intensity signal increased and that of the higher intensity signal decreased until equilibrium was reached. At an equilibrium temperature of 333 K, the diastereomeric ratio changed to 1.4 : 1 (Fig. 3d). This change in relative intensity of the signals was due to the first-order transformation of the **S**–**M**/**R**–**P** to **S**–**P**/**R**–**S** diastereomers *via* 180° rotation around the C–N bond (Fig. 1), the equilibrium constant, K, being 1.4 at 333 K. The rate constants k_1 and k_{-1} for this conversion (Fig. 1) have been found by following the reversible first-order kinetics.[17] The negative slope of the straight line obtained from plotting $\ln([A]_t - [A]_{eq}/[A]_0 - [A]_{eq})$ against time yielded rate constants from which the magnitude of the rotational barrier could be obtained using the Eyring equation.[17]

The conformations of the rotational isomers of 3-(*o*-tolyl)-5-methyl-rhodanine have been determined using through-space connectivities derived from 2D-NOESY experiments. The 2D-NOESY spectrum of the compound showed a crosspeak between the *ortho*-methyl signal of the higher intensity diastereomer with the C5 methyl signal of the same diastereomer (Fig. 4). This NOE relationship is only possible for the **S**–**M** or **R**–**P** structures where the closest distance between the hydrogens of the methyl groups is found to be 3.515 Å by DFT calculations as described later. Therefore the higher intensity stereoisomer has been assigned to the **S**–**M** (or **R**–**P**) structure. Thus the kinetics followed for determination of the rate constants refer to the conversion of the **S**–**M**/**R**–**P** pair to **S**–**P**/**R**–**M**.

Table 1 Experimentally determined kinetic and thermodynamic parameters ΔG^{o} (kcal mol^{-1}), ΔH^{o} (kcal mol^{-1}) and ΔS^{o} (cal mol^{-1}) for the thermal interconversion process between the diastereomers of **3S** and **6S** determined by following the change in the ^{1}H NMR signals. Solvent: C_6D_6

Compound	T/K	ΔG^{o}/kcal mol^{-1}	ΔH^{o}/kcal mol^{-1}	ΔS^{o}/cal mol^{-1}	k_1/s^{-1}	k_{-1}/s^{-1}	$\Delta G^{\neq}$/kcal mol^{-1}
3S	333	0.24	−1.27	−4.5	1.51×10^{-6}	2.19×10^{-6}	[a]28.47
							[b]28.20
							[c]28.80
	318	0.17					
6S	333	−0.22	0.53	2.2	1.16×10^{-5}	8.37×10^{-6}	[d]27.10
							[e]27.32
							[c]27.64
	318	−0.18					
	304	−0.15					

[a] Gibbs free energy of activation for the conversion of the higher intensity diastereomer to the lower intensity one. [b] Gibbs free energy of activation for the conversion of the lower intensity diastereomer to the higher intensity one. [c] Calculated value. [d] Gibbs free energy of activation for the conversion of S–M (R–P) to S–P (R–M). [e] Gibbs free energy of activation for the conversion of S–P (R–M) to S–M (R–P).

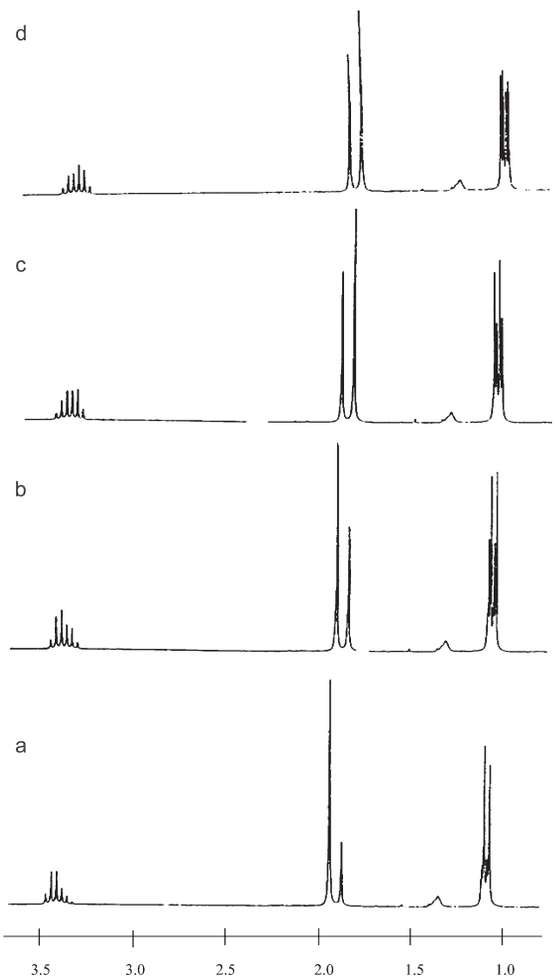

Fig. 3 250 MHz ^{1}H NMR signals of 3-(*o*-tolyl)-5-methyl-rhodanine, **6S**, for which diastereomeric signals were observed at 333 K in C_6D_6: a) at $t = 0$ s; b) $t = 9000$ s; c) $t = 83\,400$ s; d) $t = 94\,200$ s.

In the case of the 3-(*o*-chlorophenyl)-5-methyl-rhodanine (**3S**) stereoisomers, M and P conformations could not be assigned to the higher and lower intensity diastereomers because no NOE through-space connectivity could be established between the *ortho*-H and C5–H or CH_3 protons, since the proton–proton distances are of the order of *ca.* 4 Å or greater. Analysis of the reversible first-order kinetics derived from the change in the ^{1}H NMR signal for the C5–CH_3 protons yielded the rate constants and rotational barriers for this compound. The experimentally determined kinetic and thermodynamic constants for 3-(*o*-tolyl)-5-methyl-rhodanine (**6S**) and 3-(*o*-chlorophenyl)-5-methyl-rhodanine (**3S**) are summarised in Table 1.

For both **3S** and **6S** the kinetics of the thermal interconversion process have been studied by following the conversion of the higher intensity ^{1}H NMR signal to the lower intensity one. In the case of **3S** the initial higher intensity signal ended up as the thermodynamically more stable diastereomer at equilibrium. Whereas for **6S** the initial lower intensity signal turned out to be more populated at equilibrium, both **3S** and **6S** being equilibriated at 333 K, in the NMR cavity. For **6S** it is certain that the obtained kinetic and thermodynamic values (Table 1) refer to the conversion of **S**–**M** (**R**–**P**) to **S**–**P** (**R**–**M**) (Fig. 1), based on the NOESY results. However, for **3S**, since it was not possible to do the isomeric assignment, the reported k_1 and k_{-1} values are only relative.

The ΔG^{o} values, the Gibbs Free energy difference between the diastereomers, have been determined using the equilibrium constant values, $K = k_1/k_{-1}$, *via* $\Delta G^{o} = -RT\ln K$. For **6S**, the **S**–**P** (**R**–**M**) pair has been found to be slightly more stable (by about 0.2 kcal mol^{-1}) than the **S**–**M** (**R**–**P**) pair. This difference may be due to the steric repulsion between the two methyl groups in the cisoid **S**–**M** (**R**–**P**), whereas no such repulsion is present in the transoid **S**–**P** (**R**–**M**) conformations. The ΔH^{o} and ΔS^{o} values have been determined from the slope and the intercept respectively of the plot of $\ln K$ *vs.* $1/T$ assuming that ΔH^{o} and ΔS^{o} are constant over the temperature range studied.

Geometrical features

For 3-(phenyl)-5-methyl-rhodanine (**1S**), two minima, which are virtually isoenergetic, have been located on the potential energy surface at 89.0° (**1S**–**M**) and −89.3° (**1S**–**P**) (Fig. 5). The clockwise direction of the C2′–C1′–N3–C4 dihedral angle is considered as positive. In both these structures, the N lone-pair electrons are delocalized towards S7, as the C=S group is able to interact strongly with strong electron donors. The N3–C2 (1.390 Å) distance is shorter than the N3–C4 distance (1.405 Å) and C2–S7 (1.643 Å) is longer than the reference value (1.600 Å)[11] (Table 2). Transition structures (**1S**–**TS** or **1S**–**TS′**) have been located at 2.7° and 178.0° from the carbonyl side of the rhodanine plane. At these stationary, first-order saddle points, the two rings are flat and coplanar because of electron delocalization. Six-membered O8–C4–N3–C1′–C2′–H and S7–C2–N3–C1′–C6′–H rings based on electron density topology are formed by the O···H and S···H hydrogen bonds. Topological studies show that the hydrogen bonds formed between the two ring systems in these transition states are characterised by bond critical points (BCPs) of correct (3, −1) topology with a Laplacian of rho, $\nabla^2(\rho)$, which is positive and in the correct range, typical of closed-shell interactions – see discussion below. The C2′–H and C6′–H distances shorten from 1.086 Å in **1S**–**M** or **1S**–**P** to 1.076 and 1.075 Å in **1S**–**TS** and **1S**–**TS′**, respectively. Along the reaction coordinate for this transition, the positive charge on Z = H (on C6′) increases from 0.0700 a.u. (atomic units) to 0.1086 a.u. In **1S**–**TS**, electrons contribute to bonding with the neighbouring atoms (O) associated with a decrease in electron density for the hydrogen atoms bonded to C6.

In the case of 3-(*o*-fluorophenyl)-5-methyl-rhodanine (**2S**), there are two minima located on the potential energy surface at 72.8° (**2S**–**M**) and −71.9° (**2S**–**P**). These two minima are virtually isoenergetic within the calculation error, with the global minimum

Table 2 Selected geometrical parameters for the compounds **1S**, **2S**, **3S**, **4S**, **5S** and **6S** (B3LYP/6-31G*)

	C1′–N3	N3–C2	N3–C4	C2–S7	C4–O8	S1–C5	S1–C2	C2′–Z	C4–C5	C5–C6	S7–H	O8–H	C4–N3–C1′–C2′
1S–M	1.444	1.390	1.405	1.643	1.210	1.839	1.770	1.086			3.919	3.570	89.3
1S–TS	1.467	1.407	1.430	1.653	1.210	1.815	1.768	1.075				1.986	2.7
2S–M	1.434	1.391	1.406	1.642	1.209	1.840	1.768	1.345	1.527	1.533	3.539	3.957	72.8
2S–TS	1.447	1.400	1.457	1.651	1.199	1.832	1.777	1.343	1.519	1.535	2.432		−5.5
2S–TS′	1.457	1.415	1.442	1.639	1.208	1.826	1.778	1.339	1.519	1.527		2.082	172.0
3S–M	1.435	1.391	1.406	1.642	1.209	1.840	1.768	1.751	1.528	1.533	3.732	3.679	84.3
3S–TS	1.445	1.403	1.461	1.649	1.198	1.843	1.778	1.757	1.516	1.523	2.459		7.9
3S–TS′	1.456	1.414	1.453	1.636	1.205	1.831	1.786	1.751	1.517	1.526		2.184	166.7
4S–M	1.434	1.390	1.406	1.642	1.209	1.840	1.768	1.904	1.526	1.535	3.788	3.645	84.0
4S–TS	1.445	1.403	1.459	1.649	1.199	1.844	1.778	1.918	1.516	1.523	2.474		9.3
4S–TS′	1.456	1.412	1.453	1.635	1.205	1.832	1.786	1.913	1.518	1.526		2.211	164.4
5S–M	1.443	1.382	1.417	1.655	1.207	1.836	1.763	1.363	1.527	1.533	4.502	2.903	114.1
5S–TS	1.473	1.419	1.418	1.648	1.22	1.826	1.769	1.353	1.516	1.527	2.316		−4.1
5S–TS′	1.475	1.388	1.459	1.664	1.204	1.828	1.772	1.345	1.517	1.525		2.059	175.9
6S–M	1.446	1.389	1.404	1.643	1.211	1.839	1.770	1.508	1.528	1.532	3.704	3.760	82.7
6S–TS	1.461	1.403	1.447	1.651	1.203	1.838	1.778	1.517	1.518	1.524	2.411		3.7
6S–TS′	1.472	1.404	1.452	1.644	1.205	1.825	1.786	1.515	1.518	1.536		2.139	−169.5

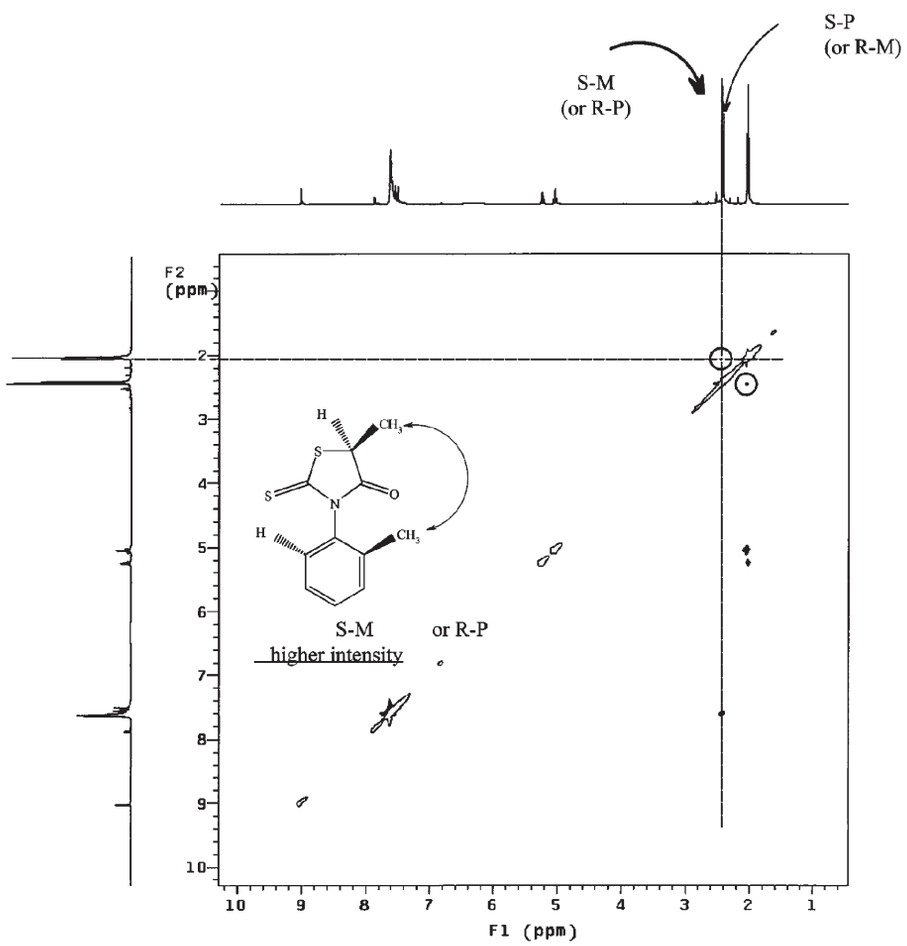

Fig. 4 2D-NOESY spectrum of 3-(*o*-tolyl)-5-methyl-rhodanine, **6S**, in pyridine-d_5 at 303 K.

2S–M being more stable than **2S–P** by *ca.* 0.04 kcal mol^{-1}. This may be due to favorable interactions between the C5 methyl group and F that are *syn* to each other at a distance of 3.207 Å. Because of favorable interactions between O and F in the transition state **2S–TS**, an inter-atomic interaction path results characterised by a (3, −1) BCP and a positive value for $\nabla^2(\rho)$, typical of a closed-shell interaction. Fluoroacetaldehyde also shows a definite preference for the *syn* conformer with the FCCO dihedral angle equal to 0°.[18] Similarly, an early experimental study by Cantacuzene and co-workers demonstrated that the axial–equatorial distribution for 2-fluorocyclohexanone was 55% in favour of the equatorial isomer.[19] In the examples cited above, special stabilizing interactions between oxygen and fluorine have been postulated. The same type of interactions would be present in $FONO_2$, whose molecular structure has been studied computationally using coupled-cluster theory.[20] In this study the molecule was found to be planar allowing an interaction between F and O. The electron density topological analysis reported in this paper provides additional evidence for a marked closed-shell interaction, in the sense defined by Bader[21] between the fluorine and oxygen atoms in the fluorophenyl-rhodanine derivative transition states studied (see Table 5 and Fig. 6). In structure **2S–M** the N3–C2 (1.391 Å) distance is shorter than the N3–C4 (1.406 Å) distance and C2–S7 (1.642 Å) is longer than the reference value 1.600 Å[10] (Table 2). The transition states for this compound are located at dihedrals corresponding to −5.5° (**2S–TS**) and 172.0° (**2S–TS′**) with the two rings nearly coplanar. **2S–TS′** (23.32 kcal mol^{-1}) is less stable than **2S–TS** (20.94 kcal mol^{-1}) because, with the dihedral equal to 172.2°, the fluorine atom is close to a sulfur atom that is less electronegative and larger than oxygen, resulting in higher steric repulsion. The thiocarbonyl group interacts with the lone pairs on

Table 3 Energetics for compounds **1S**–**6S**. ΔE^0 and ΔG^0 are the electronic and Gibbs free energies of activation with ZPE corrections (kcal mol^{-1})

Compound	C4′–N3–C1′–C2′/°	Conformation	ΔE^0	ΔG^0
1S	2.7	**1S–TS**	11.26	13.15
	89.0	**1S–M**	0.00	0.00
	178.0	**1S–TS′**	11.26	13.15
	−89.3	**1S–P**	0.00	0.00
2S	−5.5	**2S–TS**	20.94	22.53
	72.8	**2S–M**	0.00	0.00
	172.0	**2S–TS′**	23.32	24.86
	−71.9	**2S–P**	0.04	0.04
3S	7.9	**3S–TS**	27.13	28.80
	84.3	**3S–M**	0.02	0.05
	166.7	**3S–TS′**	33.42	34.90
	−83.4	**3S–P**	0.00	0.00
4S	9.3	**4S–TS**	28.32	29.90
	84.0	**4S–M**	0.00	0.00
	164.4	**4S–TS′**	34.95	36.28
	−85.8	**4S–P**	0.23	0.12
5S	−4.1	**5S–TS**	16.96	18.20
	114.1	**5S–M**	0.00	0.00
	175.9	**5S–TS′**	19.41	20.71
	−115.1	**5S–P**	0.03	0.12
6S	3.7	**6S–TS**	25.80	27.64
	82.7	**6S–M**	0.00	0.05
	−169.5	**6S–TS′**	32.10	33.73
	−83.0	**6S–P**	0.04	0.00

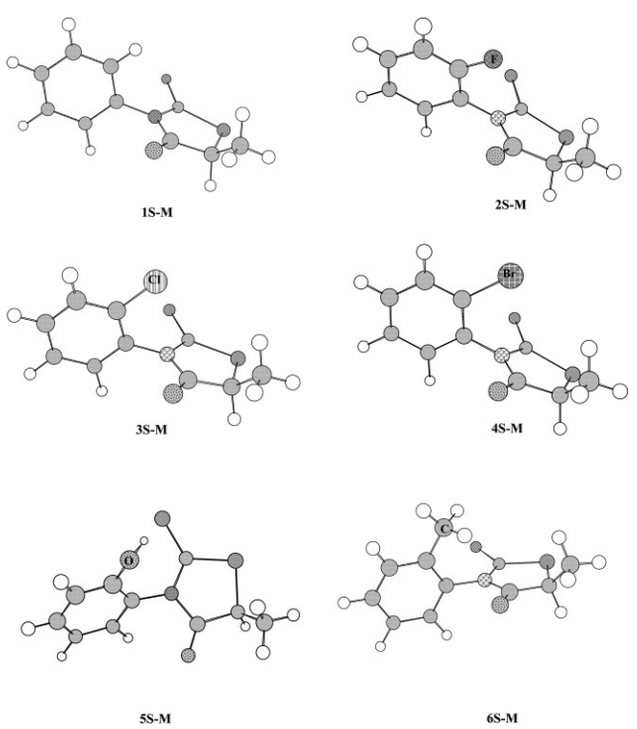

Fig. 5 Structures corresponding to the global minima for the compounds **1S** [3-(phenyl)-5-methyl-rhodanine], **2S** [3-(*o*-fluorophenyl)-5-methyl-rhodanine], **3S** [3-(*o*-chlorophenyl)-5-methyl-rhodanine], **4S** [3-(*o*-bromophenyl)-5-methyl-rhodanine], **5S** [3-(*o*-hydroxyphenyl)-5-methyl-rhodanine], **6S** [3-(*o*-tolyl)-5-methyl-rhodanine].

N3, with the result that N3–C2 is shorter than N3–C4 and C2–S7 is longer than the reference value for both **2S**–**TS** and **2S**–**TS′** structures (Table 2).

In the case of 3-(*o*-chlorophenyl)-5-methyl-rhodanine (**3S**), there are two minima located symmetrically on the potential energy surface at dihedral angles of 84.3° (**3S**–**M**) and −83.4° (**3S**–**P**). Their energies are very close to each other, however, with the minimum at −83.4° (**3S**–**P**) *ca.* 0.05 kcal mol^{-1} more stable compared to the other minimum, *i.e.* indistinguishable at the level of the calculation accuracy. Two transition structures are located at dihedrals of 7.9° (**3S**–**TS**) and 166.7° (**3S**–**TS′**), with the rings quite some way from

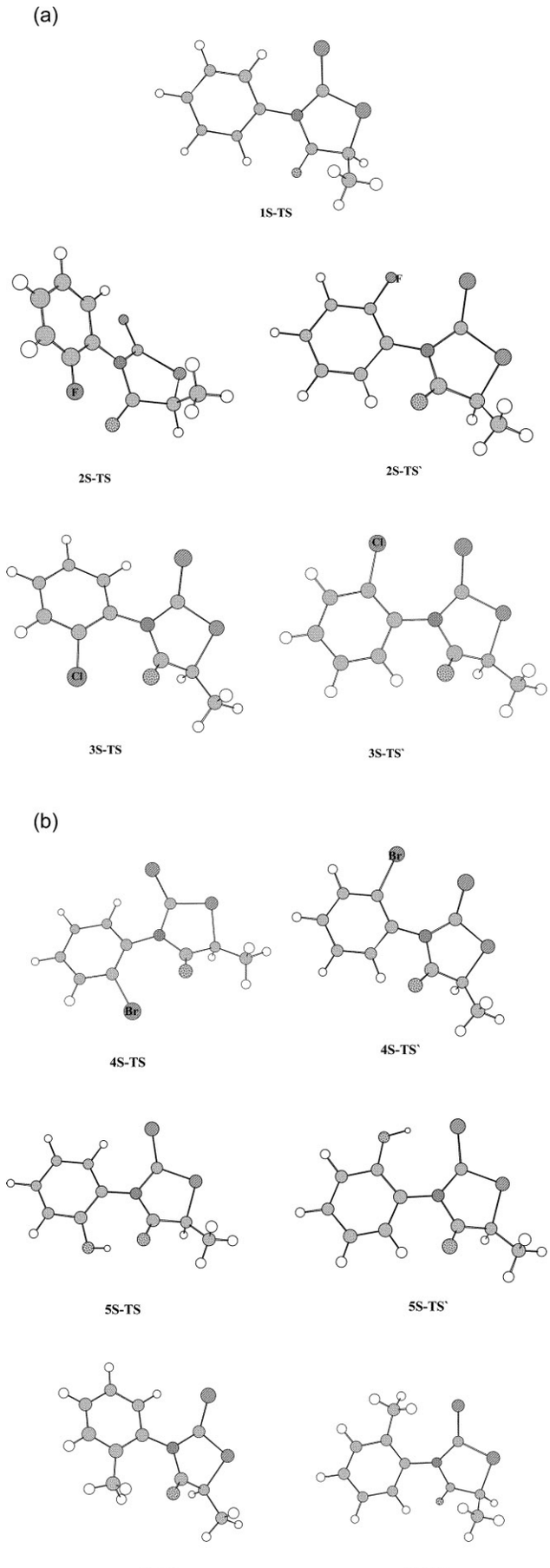

Fig. 6 Structures corresponding to the transition-state structures for the compounds **1S** [3-(phenyl)-5-methyl-rhodanine], **2S** [3-(*o*-fluorophenyl)-5-methyl-rhodanine], **3S** [3-(*o*-chlorophenyl)-5-methyl-rhodanine], **4S** [3-(*o*-bromophenyl)-5-methyl-rhodanine], **5S** [3-(*o*-hydroxyphenyl)-5-methyl-rhodanine], **6S** [3-(*o*-tolyl)-5-methyl-rhodanine].

coplanarity. The sulfur atom (S7) is larger than the oxygen (O8), so that the S7···Cl dipolar repulsion is stronger than the O8···Cl repulsion, as evidenced by larger deviations from planarity in the case of **3S**–**TS′**. As a consequence, **3S**–**TS′** has a higher rotational energy barrier than **3S**–**TS**, 33.42 kcal mol^{-1} compared to 27.13 kcal mol^{-1}, respectively. Owing to steric interactions between the sulfur and the chlorine atoms, the Cl group is pushed out of the plane of the phenyl ring. In **3S**–**TS**, N3 donates its electrons towards S7. As a result, N3–C2 (1.403 Å) is shorter than N3–C4 (1.461 Å) and C2–S7 is longer than the reference value 1.600 Å (Table 2). Two ring systems, consisting of O8–C4–N3–C1′–C2′–Cl and S7–C2–N3–C1′–C6′–H, are formed one on either side. In **3S**–**TS** the distance between H and S7 is 2.459 Å, which is suitable for H···S bonding[15] as evidenced from the topological analysis. The C2′–Cl distance lengthens from 1.751 Å (**3S**–**M**) to 1.757 Å (**3S**–**TS**). In **3S**–**TS′**, two rings, S7–C2–N3–C1′–C2′–Cl and O8–C4–N3–C1′–C6′–H, are formed one on either side. The positive charge on S7 increases from 0.0807 in **3S**–**M** to 0.3019 in **3S**–**TS′**. In **3S**–**TS′**, the S7 electrons are delocalized towards the C2–S7 bond which shortens from 1.642 to 1.636 Å (Table 2).

For the 3-(*o*-bromophenyl)-5-methyl-rhodanine, **4S**, the structure corresponding to the energy minimum located at 84.0° (**4S**–**M**) is 0.12 kcal mol^{-1} more stable than that at −85.8° (**4S**–**P**). The two transition structures are located at 9.3° (**4S**–**TS**) and 164.4° (**4S**–**TS′**). Among the substituted rhodanine compounds studied, a bromine substituent causes the largest deviation from the planarity in the transition-state structures, presumably because of its size. The bond distances for **4S**–**M** follow the same trend as those in **2S**–**M** and **3S**–**M**. In **4S**–**TS**, rings consisting of O8–C4–N3–C1′–C2′–Br and S7–C2–N3–C1′–C6′–H are formed, with (3, −1) BCPs and positive Laplacians of $\nabla^2(\rho)$ for the O···Br and H···S non-bonded interactions. The distances between O8···Br and S7···H are 2.474 and 2.839 Å, respectively. In **4S**–**TS′**, the six-membered rings S7–C2–N3–C1′–C2′–Br and O8–C4–N3–C1′–C6′–H are formed.

In 3-(*o*-hydroxyphenyl)-5-methyl-rhodanine, **5S**, the energy-minimised structure (**5S**–**M**) with a dihedral of 114.1° is 0.12 kcal mol^{-1} more stable than that with a dihedral of −115.1° (**5S**–**P**). In **5S**–**M**, the H of the OH group is tilted towards the S7 atom (C1′–C2′–O–H: 44.9°) and the O–H···S distance is 2.394 Å. In both structures the hydroxy group is directed towards the sulfur atom (S7) and away from the C5–CH_3 group ($d > 4$ Å). We have located another geometry corresponding to a stationary local minimum structure (**5S**–**M′**) in which the OH group is tilted towards the oxygen (O8) with the dihedral C4–N3–C1′–C2′ = 56.8° and C1′–C2′–O–H = −47.1°. Although **5S**–**M′** lies 0.40 kcal mol^{-1} below **5S**–**M** on the PES, it is 0.28 kcal mol^{-1} less stable on the free energy surface. In this structure the H of the hydroxy group is stabilized by O8 (O–H···O8 1.866 Å); this is confirmed by topological analysis which shows a (3, −1) BCP with a positive Laplacian – see Table 5. In **5S**–**M′** the hydrogen of the hydroxy group is in relatively close proximity to the C5–CH_3 group ($d = 3.729$ Å and $d = 3.827$ Å), destabilizing this structure on the free energy surface. The transition-state structures are located at dihedrals of −4.1° (**5S**–**TS**) and 175.9° (**5S**–**TS′**). **5S**–**TS′** (19.41 kcal mol^{-1}) is less stable than **5S**–**TS** (16.96 kcal mol^{-1}). O–H···O bonding in **5S**–**TS** is more effective than O–H···S bonding in **5S**–**TS′**,[17] as shown by electron density topological analysis. In **5S**–**TS**, the N3–C2 and N3–C4 distances are very similar. As rotation towards the carbonyl group occurs, the negative charge on O8 increases from 0.0830 a.u. to 0.2298 a.u. as a result of H-bonding. The C1′–N3 distance lengthens from 1.443 to 1.473 Å. The N3–C2 distance lengthens while N3–C4 does not change. The distance between S7···H is 2.316 Å and results in a closed-shell atomic interaction.[15] Thus a six-membered ring forms consisting of the S7–C2–N3–C1′–C6′–H atoms. The C2′–OH distance shortens from 1.363 to 1.353 Å because the OH group donates its electrons towards the C2′–OH bond. In **5S**–**TS′**, the N3–C2 bond (1.388 Å) has its shortest value. N3 donates its electrons towards S7 and, because of stabilization by S7···H–O on the C2–S7 side, N3 donation is high and the C2–S7 bond length is at its longest value compared to the other **TS′** structures (1.664 Å). Rotation towards the thiocarbonyl group causes ring formation involving O8–C4–N3–C1′–C6′–H to take place on the O8 side, O8 donating its electrons to the C6′–H bond. The O8···H5′ distance is 2.059 Å and the atoms are able to form a hydrogen bond interaction.

For the 3-(*o*-tolyl)-5-methyl-rhodanine (**6S**), the minimum with a dihedral of 82.7° (**6S**–**M**) is 0.05 kcal mol^{-1} less stable than the global minimum (**6S**–**P**). Transition structures are located at dihedrals of 3.7° (**6S**–**TS**) and −169.5° (**6S**–**TS′**). In **6S**–**TS′**, owing to the bulkiness of the S and CH_3 groups, these two groups repel each other. In **6S**–**M** the methyl groups are 3.515 Å away from each other, whereas for **6S**–**P** this distance is 5.330 Å.

Energetics

The relative electronic energies with zero-point corrections (ΔE^0) and the Gibbs free energies (ΔG^0) for compounds **1S**–**6S** are reported with respect to the most stable minimum energy conformer (Table 3). The transition structures (**TS′**) around 180° (substituent Z faces S) exhibit higher energy barriers to rotation compared to the transition structures (**TS**) around 0° (substituent Z faces O). H, F, OH, CH_3 substituents have smaller energy barriers to rotation than Cl and Br due to delocalization of electrons in the transition structures for compounds **1S**, **2S**, **5S**, **6S**. This delocalization stabilizes the transition states and decreases the energy barriers. Owing to the size of Cl and Br, the transition structures for these substituents are not planar and the dihedral angles between the five-membered heterocycle and the phenyl ring are larger (*ca.* 10°) than those for Z = H, F, OH and CH_3 (*ca.* 4°).

If only the atomic size were to be taken into account, the energy barrier to rotation would be expected to increase with the substituents in the order H, F, Cl, Br, OH, CH_3. The actual order is, however, H, OH, F, CH_3, Cl and Br. In compound **6S** the C5–CH_3···H–CH_2 distance is 4.100 Å for **6S**–**TS**, in compound **3S** the C5–CH_3···Cl distance is 4.885 Å, in **3S**–**TS** and in **4S** the C5–CH_3···Br distance is 4.936 Å in **4S**–**TS**. Although the destabilizing interactions are higher in **6S**–**TS**, the barrier is lower than expected. The order of dipole repulsion is in agreement with the above result. The dipolar repulsion for either O···Br or O···Cl is higher than for O···CH_3. In compound **5S** (Z = OH), the H bonding observed between the carbonyl group and the OH substituent stabilizes the transition state. The experimentally determined rotational energy barriers for **3S** and **6S** are 28.47 and 27.03 kcal mol^{-1}, respectively (Table 3). These energy barriers are for the rotation of the Z group from the less sterically crowded environment containing carbonyl group (C4–O8). This refers to the **TS** approached from the carbonyl side. Our calculations have shown that the free energy of activation for these compounds is 28.80 and 27.64 kcal mol^{-1}, in good agreement with the experimental results. Thus B3LYP/6-31G* can be used with confidence for the calculation of the free energy barriers in 3-(*o*-aryl)-5-methyl-rhodanines.

NBO analysis

Natural bond orbital (NBO) analysis originated as a technique for studying hybridization and covalency effects in polyatomic wave functions, based on local block eigenvectors of the one-particle density matrix.[16a] The filled NBOs are well adapted to describing covalency effects in molecules; the antibonds represent unused valence-shell capacity. Small occupancies of the antibonds correspond to small, non-covalent corrections to the picture of localized covalent bonds. The energy associated with the antibonds can be numerically assessed by deleting these orbitals from the basis-set and recalculating the total energy to determine the associated variational energy lowering.[16b] In this way one obtains a decomposition of the total energy into components associated with covalent and non-covalent contributions. Hyperconjugative interactions play a highly important role in NBO analysis. They represent the weak departures from a strictly localized natural Lewis structure. Energy stabilizations are examined in terms of delocalizations of electron density from almost filled orbitals to neighboring almost empty orbitals.[16c] Energy effects of delocalizations are expressed

Table 4 NBO energies (kcal mol^{-1}) corresponding to the main interactions in compounds **1S–TS**, **2S–TS**, **2S–TS′**, **5S–TS**, **5S–TS′**

	1S–TS	2S–TS	2S–TS′	5S–TS	5S–TS′
lpS1→σ*(C2–S7)	34.63	32.70	31.93	33.32	33.06
lpS7→σ*(S1–C2)	10.29	10.73	10.45	10.26	11.11
lpS7→σ*(C2–N3)	3.30	13.74	15.92	14.25	7.00
lpO8→σ*(C5–C4)	19.83	20.39	20.42	20.59	20.59
lpO8→σ*(C4–N3)	30.35	35.65	31.80	22.58	33.54
lpN3→σ*(C2–S7)	61.27	56.24	47.64	—	—
lpN3→σ*(C1′–C2′)	23.21	27.66	26.79	—	—
lpN3→σ*(C4–O8)	42.75	19.41	27.65	—	—
lpC2′→σ*(C1′–N3)				446.05	
lpC2′→σ*(C3′–C4′)				51.85	
lpO(OH)→lp(C2′)				48.3	
lpC6′→σ*(C1′–N3)					487.98
lpC2′→σ*(C4′–C5′)					50.44
lpO(OH)→lp(C6′)					60.51

as perturbations to the Fock matrix. In the present work, delocalizations with lone pairs as donors are considered, Table 4. In the transition structures for the compounds of interest, the electron flow in the thiazolidine structure is from the lone-electron pairs on S1 towards the C2–S7 antibonding orbitals, resulting in the elegation of this bond as seen in Table 2. The repulsion of the two rings which causes an elongation of the C1′–N3 bond is due to different factors based on the nature of the Z substituent. In the case of compounds **1S–TS**, **2S–TS** and **2S–TS′** the lone pairs on nitrogen interact with the vicinal antibonding orbitals; however, when Z = OH (**5S–TS** and **5S–TS′**) the elongation of the C1′–N3 bond is due to the interactions of the hydroxy group with the vicinal antibonding orbitals. The C1′–N3 bond length is 1.467, 1.447, 1.457, 1.473 and 1.475 Å in the compounds **1S–TS**, **2S–TS**, **2S–TS′**, **5S–TS** and **5S–TS′**, respectively. The highly-pronounced delocalization of electrons towards the σ*(C1′–N3) bond stabilizes **5S–TS** and **5S–TS′** and justifies the relatively low rotational barriers for compound **5S** as compared to **2S**.

Electron density topological analysis

We have analysed and characterised the electron density topology of all the transition states discussed above using Biegler-König's AIM2000 and Popelier's MORPHY98 programs,[14,15] as described in the Methodology section. The electron density (ρ) and the value of the Laplacian of (ρ), $\nabla^2(\rho)$, are shown together with relevant geometrical data, for both rotational transition states for each of the six title compounds studied, in Table 5. Typical electron density maps through the plane of the two ring systems are shown for the 3-(*o*-fluorophenyl)-5-methyl-rhodanine [structures **2S–TS** and **2S–TS′** – Fig. 7(a) and (b)] and for 3-(*o*-hydroxyphenyl)-5-methyl-rhodanine [structures **5S–TS** and **5S–TS′** - Fig. 7(c) and (d)]. Electron density contour plots are shown with contours plotted at 0.001, 0.002, 0.004, 0.080, 0.020… atomic units (a.u.). Molecular graphs for the 3-(*o*-fluorophenyl)- and 3-(*o*-hydroxyphenyl)-5-methyl-rhodanine transition states are shown in Fig. 8(a–d).

The non-bonded closed-shell interactions can be separated into two distinct categories. The first consists of a classical hydrogen bond between the activated *ortho*-hydrogen on the aromatic ring and either the sulfur or oxygen substituent on the five-membered thiazolidine ring. The values for the electron density and its Laplacian at the (3, −1) bond critical point (BCP), together with the geometrical parameters d and θ, indicate moderately strong hydrogen bonding comparable to that observed for the water dimer, for 1 : 1 water–ethanediol complexes or hydrated glucopyranose.[22]

The second type of non-bonded interaction is characterised by a BCP of (3, −1) topology and a positive value for its Laplacian, occurring between the *o*-aryl substituent, *i.e.* H, F, Cl, Br, OH or CH_3, and either the sulfur or oxygen atom on the thiazolidine ring, depending on the transition state. These interactions show similar values of electron density, (ρ), and its Laplacian, $\nabla^2(\rho)$, to the H···O or H···S interactions, with the exception of the 3-(*o*-hydroxyphenyl) compound, in which the O···H–O or S···H–O separation distance is much shorter, associated with a higher value for the electron density and its Laplacian.

Calculated values for the 'hydrogen bond energy', derived from the properties of the (3, −1) BCP, which are predominantly electrostatic in origin,[23] are shown in Table 6. As would be expected, the H···S interaction is somewhat weaker than that for H···O, with significant structural effects dependent on the substitution of the aromatic ring.

We used both atomic basin integration and natural bond orbital (NBO) analysis of the antibonding orbital electron occupancies to analyse further the quantitative charge transfer involved in these non-covalent interactions. The NBO results have been discussed in the previous section. Atomic basin integration was carried out using MORPHY98 [14] and AIM2000 [15] software, yielding values for the atomic charge (actually the first electrostatic moment derived from a Buckingham-type multipole analysis rather than single-point atomic charges), $q(\Omega)$, the dipolar polarisation, $\mu(\Omega)$, and the atomic volume, vol(Ω). Both the atomic charge, $q(\Omega)$, and the atomic volume, vol(Ω), were estimated out to the 0.001 a.u. electron density contour. The values obtained are shown in Table 7 for the six title compounds studied.

Charges derived by AIM theory atomic basin integration have been shown to be amongst the most accurate and to be preferred over other methods.[22,24] Mulliken charges are not as useful and are markedly dependent on the basis-set but less so on the correlation functional used, with 6-31+G(d) giving higher charges than 6-311+G(2d,p). Charges derived from atomic basin integration are more stable, showing variations in the third or fourth significant figure for the different levels of theory.[22] Guerra *et al.*[25] have pointed out recently that both the AIM and NPA electron density partitioning schemes seem to yield unrealistically large atomic charges, especially for oxygen, implying a greater ionic character than is 'chemically reasonable', in comparison to the Hirshfeld or Voronoi deformation density procedures, which these authors prefer. Nonetheless, charges derived from the use of the AIM partitioning scheme can be recommended for comparative purposes, as in the present case, where changes in charge distribution, *i.e.* charge transfer, rather than absolute values are important. Values for the two starting structures in each case are shown as an average since these were found to be substantially conformer-independent, with differences being observed only in the fourth or fifth significant figure.

A comparison of the 3-(*o*-fluorophenyl)-, 3-(*o*-chlorophenyl)- and 3-(*o*-bromophenyl)-5-methyl-rhodanine transition state structures for compounds **2S**, **3S**, **4S** is instructive. The dipolar polarisation, $\mu(\Omega)$, of the sulfur and oxygen atoms attached to the thiazolidine ring is markedly greater in either **TS** or **TS′** as compared to the reference values, 0.8902 ± 0.0225 and 0.4573 ± 0.0053 a.u., respectively. The dipolar polarisation for the oxygen atom increases when it interacts with the halogen rather than with the aromatic *ortho*-hydrogen atom by +0.0516 a.u. (F); +0.0276 a.u. (Cl); and +0.0221 a.u. (Br). This is also true for the sulfur atom: +0.0204 a.u. (F); +0.0137 a.u. (Cl); +0.0076 a.u. (Br). The aromatic *ortho*-hydrogen, on the other hand, shows

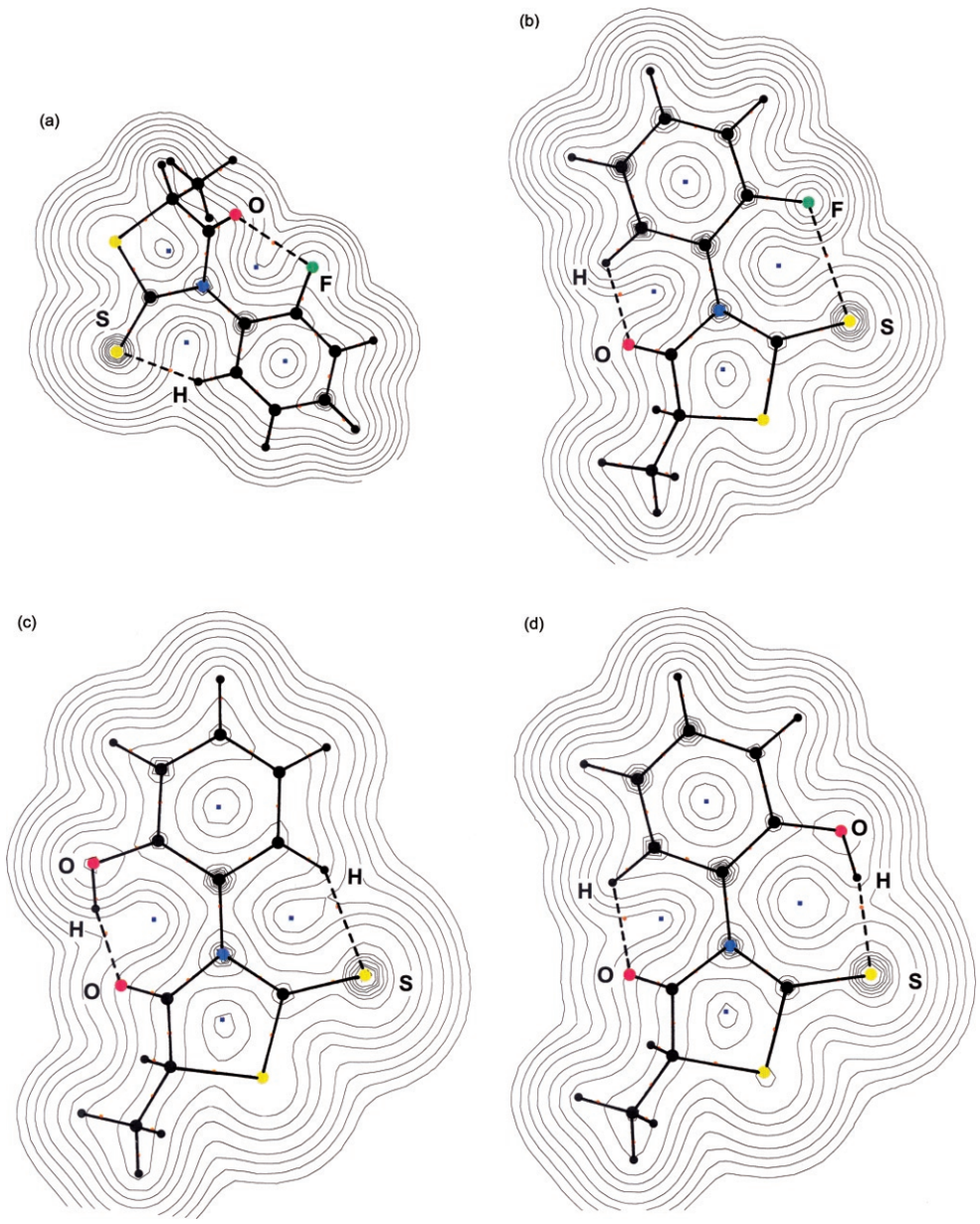

Fig. 7 Electron density contour maps through the plane of the rings for the transition states **TS** and **TS′** for 3-(*o*-fluorophenyl)-5-methyl-rhodanine (**2S**) [(a) and (b)], and for 3-(*o*-hydroxyphenyl)-5-methyl-rhodanine (**5S**) [(c) and (d)]. Electron denisty contours are shown at 0.001, 0.002, 0.004, 0.008, 0.020, 0.040… a.u. Atoms are colour coded (carbon, hydrogen = black; oxygen = red; nitrogen = blue; halogens = green or brown).

a reduction in dipolar polarisation compared to the reference value of 0.1413 ± 0.0007 a.u. when it interacts with oxygen or sulfur, corresponding to observations in other hydrogen-bonded systems.[21] The difference in *ortho*-hydrogen dipole polarisation between H···O and H···S is influenced by the *o*-halogen substituent, *i.e.* +0.0128 a.u. (F); +0.0086 a.u. (Cl); and +0.0065 a.u. (Br). Upon interaction, oxygen becomes more negatively charged and sulfur more positively charged compared to the reference values of −1.1263 ± 0.0035 and +0.0787 ± 0.0041 a.u., respectively, the larger numerical values being associated with interaction with the *o*-halogen in the order F > Cl > Br. The other feature highlighted by the data in Table 7 is that the atomic volume decreases sharply upon non-covalent interaction and this is reflected in marked increases in the average nuclear charge density [data not shown but equal to $q(\Omega)/\mathrm{vol}(\Omega)$].

The *o*-hydroxyphenyl-derivative is characterised by a **TS** with a short, strong, hydrogen bond between the OH hydrogen and the rhodanine oxygen atom, with values for the electron density, (ρ), and its Laplacian, $\nabla^2(\rho)$, at the bond critical point of 0.0563 and +0.1956 a.u., respectively, and an O–H···O distance of 1.61 Å (see Table 5). The OH hydrogen atom in **5S**–**TS** has increased positive charge (0.0351 a.u.) and a considerably reduced dipolar polarisation (−0.0313 a.u.), together with a marked diminution in atomic volume, all of which are typical for the *+…*− charge transfer seen in strong hydrogen bonding.[22] In **5S**–**TS′**, in which the OH group is hydrogen bonded to the sulfur atom, these effects are qualitatively similar but smaller in magnitude.

Conclusions

Our results demonstrate very clearly that the quasi-planar transition structures for the rotational equilibrium around the C–N bond joining the two ring systems in the *o*-aryl-substituted 5-methyl-rhodanines studied, are stabilized by non-bonded, closed-shell interactions between the *o*-substituent, Z = H, F, Cl, Br, OH and CH_3, and the *o*-hydrogen atom with the pendant S and O atoms of the rhodanine ring; these interactions are characterised by (3, −1) BCPs and positive values for Laplacian of the electron density at the critical point, thus satisfying Bader's criteria for the closed-shell type.[21] It is interesting to note that, in the much simpler unsubstituted biphenyl system, a transition state also exists in which the two rings are coplanar and stabilized by H···H non-bonded interactions which are of the closed-shell variety with a (3, −1) BCP and a positive value for the Laplacian of the electron density

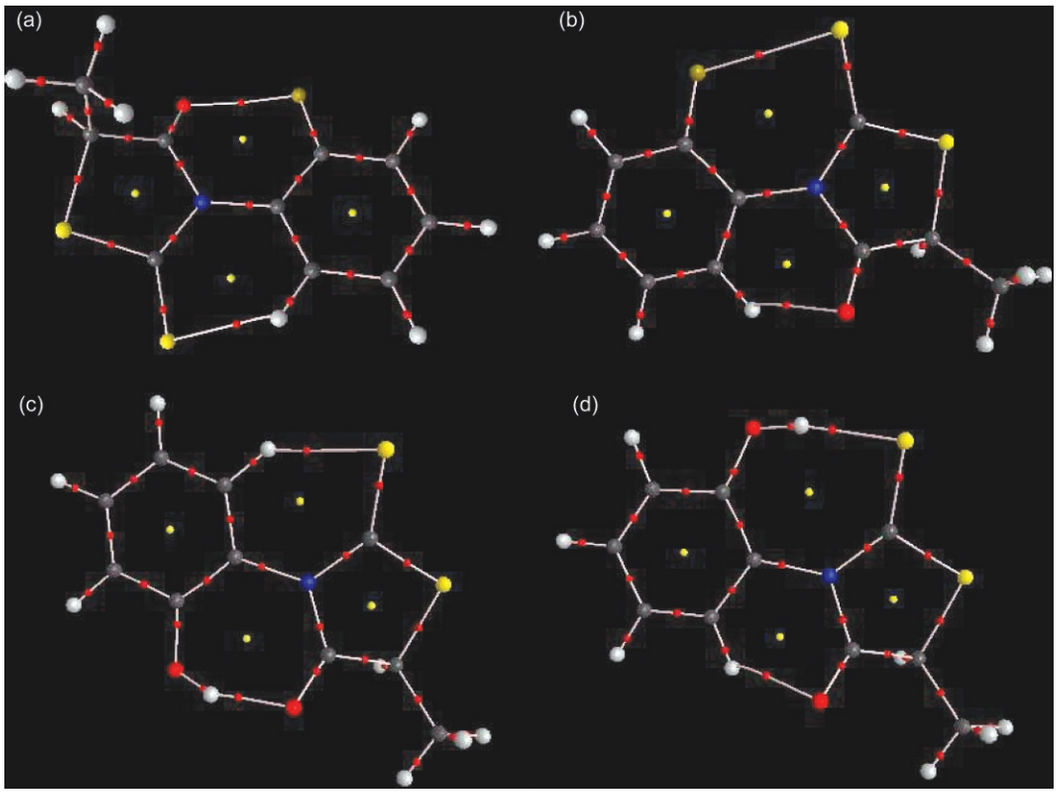

Fig. 8 Molecular graphs for the same structures as in Fig. 7(a–d). BCPs are shown as small red dots and RCPs as yellow dots.

at the critical point [$\rho = 0.0155$ a.u.; (ρ), $\nabla^2(\rho) = +0.0607$ a.u.]. The energy difference between the coplanar transition state and the global energy minimum in which the two benzene rings are orthogonal to one another is approximately 2.5–3.0 kcal mol^{-1} (R. A. Klein, unpublished data). Although surprising at first glance, hydrogen–hydrogen interactions, which appear to stabilize the coplanar biphenyl transition state, have been described as the 'di-hydrogen bond' in other systems.[26]

Detailed analysis of these non-bonded, closed-shell interactions using atomic basin integration techniques together with NBO analysis, has provided insights into the nature of these interactions and the role of charge transfer. Of particular interest are the interactions between sulfur and oxygen with the halogens, fluorine, chlorine and bromine, as discussed in the previous section. There is both experimental and theoretical evidence in the literature for oxygen–oxygen non-bonded closed-shell interactions in inter- and intra-molecular complexes.[27,28] Evidence is also available for similar fluorine–fluorine interactions.[29]

Although the presence of a (3,−1) bond critical point (BCP) and an inter-atomic bond path in a structure at its electrostatic equilibrium goemetry has been considered[30] to be proof of a bonding interaction, it seems implausible chemically to classify the closed-shell interactions described above as bonding in the classical sense. Rather they are quantum-mechanical interactions between the electron distributions of the atoms involved which possess topological properties shared by classically bonded systems but are of the closed-shell type with a positive Laplacian of the electron density (ρ), $\nabla^2(\rho)$, at the BCP and interaction energies at least an order of magnitude smaller than for a 'normal' covalent bond. It is these interactions that stabilize the rotational transition states studied in this paper.

Calculation of the height of the barriers to rotation using B3LYP/6-31G* gives results which are in remarkably good agreement with those obtained experimentally using NMR spectroscopy, supporting the use of computationally efficient DFT methods for problems of this type.

References

1 B. C. C. Contello, M. A. Cawhorne, D. Haigh, R. M. Hindley, S. A. Smith and P. L. Thurlby, *Bioorg. Med. Chem. Lett.*, 1994, **4**, 1181–1184.

2 B. C. C. Contello, D. S. Eggleston, D. Haigh, R. C. Haltiwanger, C. M. Heath, R. M. Hindley, K. R. Jennings, J. T. Sime and S. R.Woroneicki, *J. Chem. Soc. Perkin Trans. 1*, 1994, 3319–3324.

3 *Internal Rotation in Molecules*, W. J. Orville-Thomas, ed., John Wiley and Sons, New York, 1974, pp. 1–7.

4 R. S. Cahn, C. K. Ingold and V. Prelog, *Angew. Chem., Int. Ed.*, 1966, **5**, 385.

5 I. Dogan, N. Pustet and A. Mannschreck, *J. Chem. Soc., Perkin Trans. 2*, 1993, 1957–1560.

6 L. D. Colebrook, *Can. J. Chem.*, 1990, **69**, 1957–1963.

7 C. Roussel, W. A. König and C. Wolf, *Liebigs Ann.*, 1995, 781–786.

8 C. Roussel, W. A. König and C. Wolf, *Liebigs Ann.*, 1996, 357–363.

9 C. Cui, J. Cho, S. J. Kim, C. J. Jung and C. Baehr, *J. Chem. Phys.*, 1997, **107**(23), 10 201–10 206.

10 K. Rang, F. L. Liao, J. Sandstrom and S. L. Wang, *J. Chem. Soc., Perkin Trans. 2*, 1995, 1521–1524.

11 I. Dogan, T. Burgemeister, S. Içli and A. Mannschreck, *Tetrahedron*, 1992, **48**(35), 7157–7164.

12 *SPARTAN Version 5.1.1*, Wavefunction, Inc., California, 1997.

13 M. J. Frisch, G. W. Trucks, H. B. Schlegel, G. E. Scuseria, M. A. Robb, J. R. Cheeseman, V. G. Zakrzewski, J. A. Montgomery, Jr., R. E. Stratmann, J. C. Burant, S. Dapprich, J. M. Millam, A. D. Daniels, K. N. Kudin, M. C. Strain, O. Farkas, J. Tomasi, V. Barone, M. Cossi, R. Cammi, B. Mennucci, C. Pomelli, C. Adamo, S. Clifford, J. Ochterski, G. A. Petersson, P. Y. Ayala, Q. Cui, K. Morokuma, D. K. Malick, A. D. Rabuck, K. Raghavachari, J. B. Foresman, J. Cioslowski, J. V. Ortiz, A. G. Baboul, B. B. Stefanov, G. Liu, A. Liashenko, P. Piskorz, I. Komaromi, R. Gomperts, R. L. Martin, D. J. Fox, T. Keith, M. A. Al-Laham, C. Y. Peng, A. Nanayakkara, C. Gonzalez, M. Challacombe, P. M. W. Gill, B. Johnson, W. Chen, M. W. Wong, J. L. Andres, C. Gonzalez, M. Head-Gordon, E. S. Replogle and J. A. Pople, *Gaussian-98 Revision A.7*, Gaussian Inc., Pittsburgh PA, 1998.

14 *MORPHY98*, a topological analysis program written by P. L. A. Popelier with a contribution from R. G. A. Bone (UMIST, Engl., EU); P. L. A. Popelier, *Comput. Phys. Commun.*, 1996, **93**, 212; P. L. A. Popelier, *Theor. Chim. Acta*, 1994, **87**, 465; P. L. A. Popelier, *Mol. Phys.*, 1996, **87**, 1169; P. L. A. Popelier, *Comput. Phys. Commun.*, 1998, **108**, 180; P. L. A. Popelier, *Can. J. Chem.*, 1996, **74**, 829.

15 F. Biegler-König, *J. Comput. Chem.*, 2000, **21**, 1040; F. Biegler-König, J. Schönbohm and D. Bayles, *J. Comput. Chem.*, 2001, **22**, 545.

16 (*a*) J. P. Foster and F. Weinhold, *J. Am. Chem. Soc.*, 1980, **102**, 7211–7218; (*b*) A. E. Reed, L. A. Curtiss and F. Weinhold, *Chem. Rev.*, 1988, **88**, 899; (*c*) J. T. Blair and J. Stevens, *Heterocycles*, 1994, **37**, 1473.

17 I. N. Levine, *Physical Chemistry*, McGraw-Hill, New York, 1995, p. 503.

18 J. R. Durig and H. V. Phan, *J. Mol. Struct. (THEOCHEM)*, 1990, **209**, 333–347.

Table 5 Electron density topological properties of the non-covalent interactions in the transition-state structures discussed in the text. Electron density (ρ) and the Laplacian of (ρ), $\nabla^2(\rho)$ at the (3, −1) BCP are shown in atomic units (a.u.) The dihedral angle, Φ, in degrees, is defined as C2′–C1′–N–C4, θ as C–Z···O or S; the distance between interacting nuclei, d, is given in Å

	TS								**TS′**							
	Z···O				H···S				Z···S				H···O			
Compounds	(ρ)	$\nabla^2(\rho)$	d	θ	(ρ)	$\nabla^2(\rho)$	d	θ	Φ	(ρ)	$\nabla^2(\rho)$	d	θ	(ρ)	$\nabla^2(\rho)$	d	θ	Φ
o-phenyl- (**1S**)	0.0219	0.1062	1.986	122.9	0.0248	0.0730	2.31	132.5	2.7	—	—	—	—	—	—	—	—	—
o-fluorophenyl- (**2S**)	0.0229	0.0967	2.428	107.5	0.0195	0.0641	2.43	123.9	−5.5	0.0215	0.0783	2.734	114.7	0.0230	0.0929	2.082	117.7	172.0
o-chlorophenyl- (**3S**)	0.0201	0.0790	2.757	90.8	0.0186	0.0638	2.45	120.8	8.0	0.0181	0.0635	3.107	96.9	0.0199	0.0872	2.183	112.0	166.6
o-bromophenyl- (**4S**)	0.0204	0.0721	2.838	85.7	0.0182	0.0634	2.47	119.3	9.3	0.0187	0.0577	3.188	91.5	0.0195	0.0866	2.211	110.2	164.4
o-hydroxyphenyl- (**5S**)	0.0563	0.1956	1.606	154.8	0.0241	0.0728	2.31	132.4	−4.1	0.0482	0.0894	1.953	168.0	0.0238	0.9571	2.051	120.6	175.9
o-tolyl- (**6S**)	0.0194	0.0803	2.224	102.2	0.0202	0.0666	2.40	124.7	3.8	0.0160	0.0585	2.636	103.8	0.0212	0.0909	2.138	114.7	190.5

Table 6 Electrostatic interaction energies (kcal mol^{-1}) calculated from the properties of the (3, −1) bond critical point (BCP) as described in the text

Compound	H···S	H···O	O···Z	S···Z
1S	−5.97	−7.60	—	—
2S	−4.37	−5.98	−6.76	−5.92
3S	−4.10	−4.89	−4.87	−3.89
4S	−3.98	−4.70	−4.47	−3.55
5S	−5.81	−6.24	−16.84	−11.98
6S	−4.61	−5.34	−4.66	−3.17

19 D. Ricard, R. Jantzen and J. Cantacuzene, *Tetrahedron*, 1972, **28**, 717–734.

20 J. T. Lee, *J. Phys. Chem.*, 1995, **99**, 1943–1948.

21 R. F. W. Bader, *Atoms in Molecules: A Quantum Theory* (The International Series of Monographs on Chemistry, No. 22), Clarendon Press, Oxford, 1990, 438 pp.

22 R. A. Klein, *J. Comput. Chem.*, 2002, **23**(6), 585–599; R. A. Klein, *J. Am. Chem. Soc.*, 2002, **124**(46), 13 931–13 937; R. A. Klein, *J. Comput. Chem.*, 2003, **24**(9), 1120–1131 and refs. cited in all of these papers.

23 E. Espinosa, E. Molins and C. LeComte, *Chem. Phys. Lett.*, 1998, **285**, 170–173; E. Espinosa, C. LeComte and E. Molins, *Chem. Phys. Lett.*, 1999, **300**, 745–748; E. Espinosa, M. Souhassou, H. Lachekar and C. LeComte, *Acta Crystallogr., Sect. B*, 1999, **55**, 563–572; E. Espinosa and E. Molins, *J. Chem. Phys.*, 2000, **113**, 5686–5694; P. Coppens, Y. Abramov, M. Carducci, B. Korjov, I. Novozhilova, C. Alhambra and M. R. Pressprich, *J. Am. Chem. Soc.*, 1999, **121**, 2585–2593.

24 K. B. Wiberg and P. R. Rablen, *J. Comput. Chem.*, 1993, **14**(12), 1504–1518.

25 C. F. Guerra, J.-W. Handgraaf, E. J. Baerends and F. M. Bickelhaupt, *J. Comput. Chem.*, 2003, **25**(2), 189.

26 E. Peris, J. C. Lee, J. R. Rambo, O. Einstein and R. H. Crabtree, *J. Am. Chem. Soc.*, 1995, **117**, 3485; R. H. Crabtree, *Science*, 1998, **282**, 2000; S. A. Kulkarni, *J. Phys. Chem. A*, 1998, **102**, 7704; I. Alkorta, I. Rozas and J. Elguero, *Chem. Soc. Rev.*, 1998, **27**, 163; S. J. Grabowski, *Chem. Phys. Lett.*, 2000, **327**, 203; R. Custelcean and J. E. Jackson, *Chem. Rev.*, 2001, **101**, 1963; I. Alkorta, J. Elguero, O. Mó, M. Yanez and J. E. Del Bene, *J. Phys. Chem. A*, 2002, **106**, 9325.

27 G. V. Gibbs, M. B. Boisen, K. M. Rosso, D. M. Tetr and M. S. T. Bukowinski, *J. Phys. Chem. B*, 2000, **104**, 10 534; A. Bach, D. Lentz and P. Luger, *J. Phys. Chem. A*, 2001, **105**, 7405; E. A. Zhurova, V. G. Tsirelson, A. I. Stash and A. Pinkerton, *J. Am. Chem. Soc.*, 2002, **124**, 4574.

28 J. Cioslowski, L. Edgington and B. B. Stefanov, *J. Am. Chem. Soc.*, 1991, **113**, 4751; J. M. Bofill, S. Olivella, A. Solé and J. M. Anglada, *J. Amr. Chem. Soc.*, 1999, **121**, 1337; I. Alkorta and J. Elguero, *J. Chem. Phys.*, 2002, **117**, 6463.

29 J. Cioslowski, L. Edgington and B. B. Stefanov, *J. Am. Chem. Soc.*, 1995, **117**, 10 381; I. Alkorta and J. Elguero, *J. Am. Chem. Soc.*, 2002, **124**, 1488; I. Alkorta and J. Elguero, *Struct. Chem.*, 2004, **15**, 117; I. Hargittai, *The Structure of Volatile Sulfur Compounds*, Reidel, Dordrecht, 1985.

30 R. F. W. Bader, *J. Phys. Chem. A*, 1998, **102**, 7314.

Table 7 Atomic basin integration for the interacting atoms in the compounds studied: atomic charge, $q(\Omega)$; dipole polarisation, $\mu(\Omega)$; and atomic volume, vol(Σ), are given, in atomic units

	S	O	H	Z
1S–TS (1S–TS′)				
$q(\Omega)$	0.2192	−1.1714	0.1086	0.1193
$\mu(\Omega)$	1.1712	0.5761	0.1291	0.1216
vol(Ω)	219.29	118.38	35.70	34.73
1S–M				
$q(\Omega)$	0.0737	−1.1293	0.0700	0.0701
$\mu(\Omega)$	0.8986	0.4540	0.1425	0.1425
vol(Ω)	233.58	133.09	47.07	47.58
2S–TS				
$q(\Omega)$	0.2216	−1.1319	0.1006	−0.6404
$\mu(\Omega)$	1.1693	0.6420	0.1395	0.3274
vol(Ω)	221.85	117.76	37.47	92.61
2S–TS′				
$q(\Omega)$	0.3070	−1.1654	0.0938	−0.6559
$\mu(\Omega)$	1.1897	0.5904	0.1267	0.3192
vol(Ω)	214.15	118.29	36.76	94.43
2S–M				
$q(\Omega)$	0.0772	−1.1248	0.0805	−0.6493
$\mu(\Omega)$	0.8980	0.4562	0.1409	0.2717
vol(Ω)	232.51	131.37	46.67	107.73
3S–TS				
$q(\Omega)$	0.2282	−1.1424	0.0874	−0.1793
$\mu(\Omega)$	1.1718	0.6308	0.1398	0.1891
vol(Ω)	222.15	117.37	38.00	198.42
3S–TS′				
$q(\Omega)$	0.3019	−1.1592	0.0719	−0.1808
$\mu(\Omega)$	0.8999	0.6032	0.1312	0.1777
vol(Ω)	214.84	118.96	38.46	199.01
3S–M				
$q(\Omega)$	0.0807	−1.1275	0.0786	−0.1818
$\mu(\Omega)$	0.8999	0.4573	0.1409	0.1735
vol(Ω)	233.35	132.45	46.61	214.57
4S–TS				
$q(\Omega)$	0.2298	−1.1471	0.0850	−0.0383
$\mu(\Omega)$	1.1726	0.6265	0.1388	0.3555
vol(Ω)	222.17	117.34	38.25	241.83
4S–TS′				
$q(\Omega)$	0.3000	−1.1591	0.0673	−0.0377
$\mu(\Omega)$	1.1802	0.6044	0.1323	0.3469
vol(Ω)	213.90	119.13	38.83	242.09
4S–M				
$q(\Omega)$	0.0830	−1.1290	0.0797	−0.0410
$\mu(\Omega)$	0.9018	0.4579	0.1407	0.3847
vol(Ω)	233.13	133.24	46.56	254.07
5S–TS				
$q(\Omega)$	0.2505	−1.1749	0.0950	0.6173
$\mu(\Omega)$	1.1740	0.5479	0.1307	0.1172
vol(Ω)	218.48	114.00	35.95	11.85
5S–TS′				
$q(\Omega)$	0.1792	−1.1543	0.0831	0.5653
$\mu(\Omega)$	1.1105	0.6062	0.1252	0.1382
vol(Ω)	215.30	117.89	36.67	14.52
5S–M				
$q(\Omega)$	0.0231	−1.1208	0.0695	0.5822
$\mu(\Omega)$	0.8443	0.4668	0.1416	0.1485
vol(Ω)	225.78	130.22	46.34	17.91
6S–TS				
$q(\Omega)$	0.2235	−1.1585	0.0834	0.0642[a]
$\mu(\Omega)$	1.1743	0.6068	0.1372	0.1356[a]
vol(Ω)	221.78	116.25	37.58	41.12[a]
6S–TS′				
$q(\Omega)$	0.2456	−1.1591	0.0696	0.0551[a]
$\mu(\Omega)$	1.1737	0.6059	0.1301	0.1452[a]
vol(Ω)	215.57	120.05	39.15	42.63[a]
6S–M				
$q(\Omega)$	0.0705	−1.1319	0.0672	0.0437[b]
$\mu(\Omega)$	0.8983	0.4513	0.1434	0.1502[b]
vol(Ω)	233.62	132.87	47.49	48.28[b]

[a] Hydrogen-bonded CH_3 hydrogen. [b] Average for all non-bonded CH_3 hydrogens.